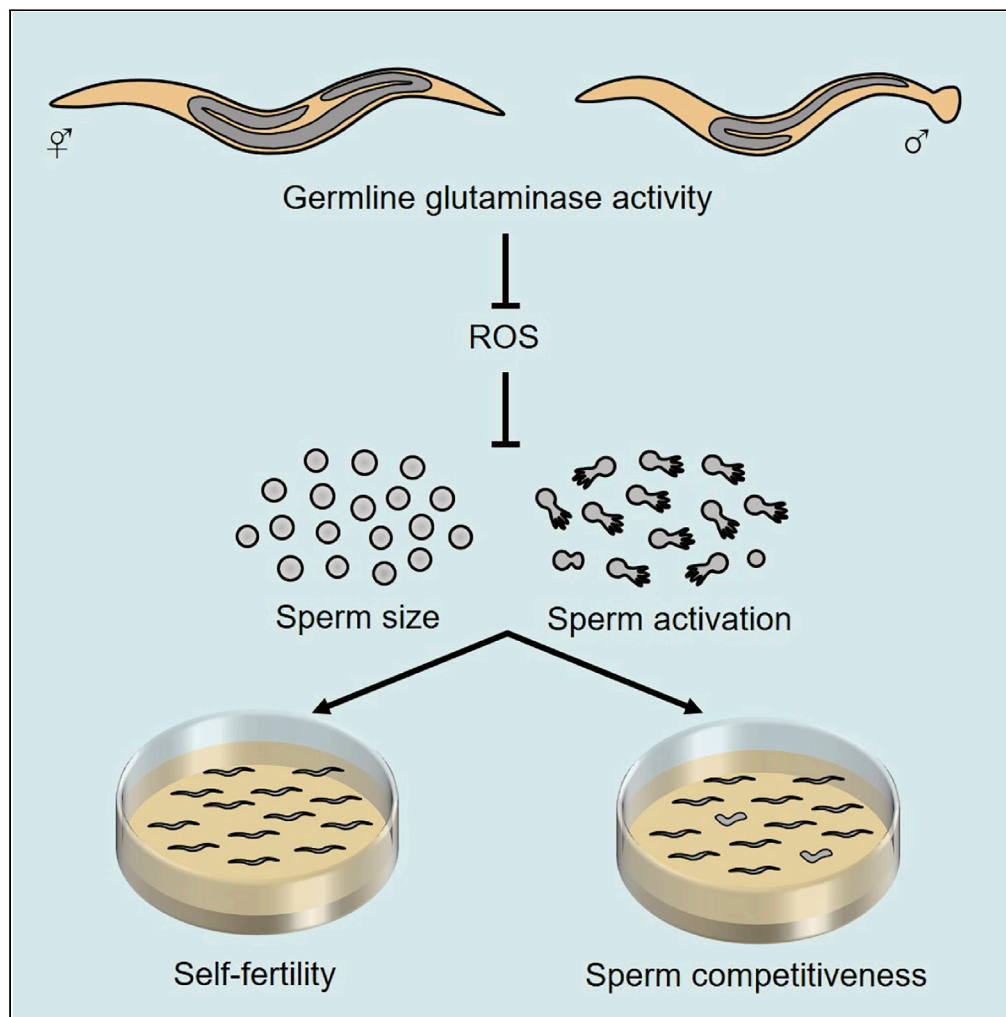**Article**

Loss of mammalian glutaminase orthologs impairs sperm function in *Caenorhabditis elegans*

Qifei Liang,
Haiyan Yang,
Zhifei Zhang, Jialin
C. Zheng, Zhao
Qin

jialinzheng@tongji.edu.cn
(J.C.Z.)
zqin.med@tongji.edu.cn (Z.Q.)

Highlights

Glutaminase gene activity
is required for optimal
sperm function in
Caenorhabditis elegans

Loss of glutaminases
reduces hermaphrodite
self-fertility and male
sperm advantage

Germline glutaminase
activity is important for
sperm function

Glutaminase promotes
sperm function by
maintaining cellular redox
homeostasis

Article

Loss of mammalian glutaminase orthologs impairs sperm function in *Caenorhabditis elegans*

Qifei Liang,[1] Haiyan Yang,[2] Zhifei Zhang,[2] Jialin C. Zheng,[1,2,3,4,*] and Zhao Qin[2,4,5,*]

SUMMARY

The decline in sperm function is a major cause of human male infertility. Glutaminase, a mitochondrial enzyme that catalyzes the hydrolysis of glutamine to generate glutamate, takes part in many diverse biological processes such as neurotransmission, metabolism, and cellular senescence. Here we report the role of glutaminase in regulating sperm function. By generating a triple mutant that harbors a loss-of-function allele for each of all three mammalian glutaminase orthologs, we found that glutaminase gene activity is required for optimal *Caenorhabditis elegans* sperm function. Tissue-specific gene manipulations showed that germline glutaminase activity plays an important role. Moreover, transcriptional profiling and antioxidant treatment suggested that glutaminase promotes sperm function by maintaining cellular redox homeostasis. As maintaining a low level of ROS is crucial to human sperm function, it is very likely that glutaminase plays a similar role in humans and therefore can be a potential target for treating human male infertility.

INTRODUCTION

Infertility has become a global public health issue for the past several decades, currently affecting one in six couples worldwide. While a lot of emphases is put on the female, male factors account for ~40% of all infertility cases and the decline in sperm quality is a major contributor to the deteriorating human fertility.[1] Moreover, it has been reported that sperm dysfunction is associated with an increase in the risk of a wide variety of genetic disorders in the offspring, including childhood cancers and neuropsychiatric diseases such as autism and schizophrenia.[2] Therefore, the identification of factors that regulate sperm function is of great importance for treating human infertility and for enhancing the fitness of the progeny.

C. elegans is a model organism that has both hermaphrodites and males, and spermatogenesis takes place in both sexes. While it persists in males, spermatogenesis finishes before the young adult stage in hermaphrodites and the sperm produced are used for self-fertilization only. Even though *C. elegans* spermatogenesis is completed without support from accessory cells, as there is no equivalent to the Sertoli cell found in mammals, it shares many common features with mammalian spermatogenesis especially during the process when spermatozoa become fertilization-competent. As a powerful genetic tool, *C. elegans* has been used to study the cell biology and genetics of spermatogenesis, in the hope of finding evolutionarily conserved mechanisms and factors.[3]

Glutaminase is a mitochondrial enzyme that catalyzes the hydrolysis of glutamine to generate glutamate. The mammalian genome encodes two glutaminase genes, *Gls1* and *Gls2*. Each produces multiple isoforms with distinct tissue distributions through alternative splicing.[4] Since glutamate is the most abundant excitatory neurotransmitter in the mammalian brain and a metabolic precursor of the inhibitory neurotransmitter GABA, the activity of glutaminase must be tightly controlled for proper brain function.[5] Besides its critical role in neurotransmission, glutaminase is involved in many aspects of cellular metabolism. Glutaminase takes part in energy production since glutamate can be converted to α-ketoglutarate which enters the tricarboxylic acid cycle to generate ATP. Glutamate also provides a source of carbon and/or nitrogen for the biosynthesis of amino acids, fatty acids, and nucleotides. In addition, glutaminase controls cellular redox homeostasis through the synthesis of glutathione.[6] Because of its pleiotropic effects on cellular metabolism, glutaminase has been implicated in tumorigenesis and become a therapeutic target in cancer therapy. Recently, it has been reported that GLS1 is a key regulator of cellular senescence. GLS1-mediated glutaminolysis increases ammonia production which neutralizes H$^+$ released by damaged lysosome in

[1]Center for Translational Neurodegeneration and Regenerative Therapy, Shanghai Tongji Hospital Affiliated to Tongji University School of Medicine, Shanghai 200072, China

[2]Key Laboratory of Spine and Spinal Cord Injury Repair and Regeneration of Ministry of Education, Orthopedic Department of Tongji Hospital, School of Medicine, Tongji University, Shanghai 200065, China

[3]Translational Research Institute of Brain and Brain-Like Intelligence, Shanghai Fourth People's Hospital Affiliated to Tongji University School of Medicine, Shanghai 200081, China

[4]Collaborative Innovation Center for Brain Science, Tongji University, Shanghai 200092, China

[5]Lead contact

*Correspondence:
jialinzheng@tongji.edu.cn
(J.C.Z.),
zqin.med@tongji.edu.cn
(Z.Q.)

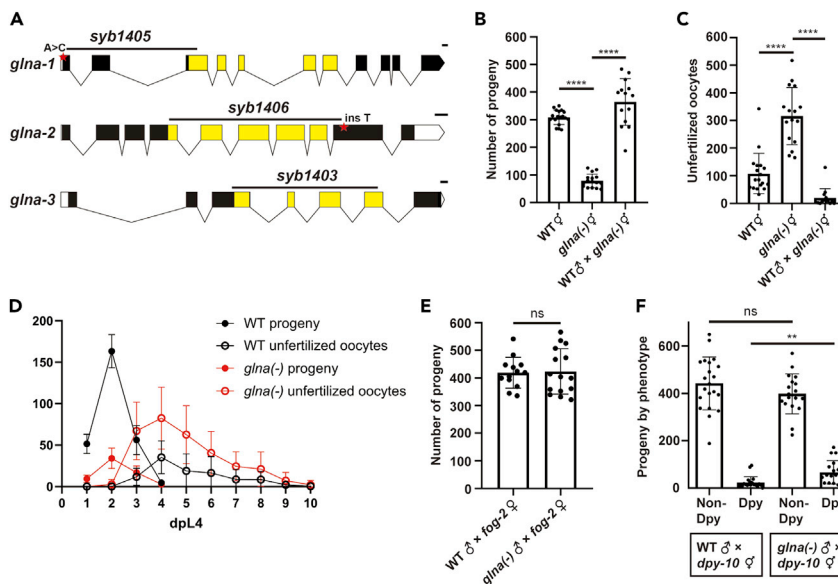https://doi.org/10.1016/j.isci.2023.106206

Figure 1. Loss of *C. elegans glna* genes reduces hermaphrodite self-fertility and male sperm competitiveness

(A) Schematics showing the genomic structure of *glna-1*, *glna-2*, and *glna-3*. Solid boxes, exons; empty boxes, UTRs; lines, introns. The conserved glutaminase catalytic domain is highlighted in yellow. The deletion and single-nucleotide change site in *glna-1(syb1405)*, *glna-2(syb1406)*, and *glna-3(syb1403)* alleles are indicated by black line and red asterisk, respectively. Scale bars, 100 bp.

(B) Number of progeny produced by self-fertile wild-type and *glna(−)* hermaphrodites, and *glna(−)* hermaphrodites crossed to wild-type young adult males.

(C) Number of unfertilized oocytes produced by animals shown in (B).

(D) Number of progeny and number of unfertilized oocytes produced on each day during their reproductive span by self-fertile wild-type and *glna(−)* hermaphrodites shown in (B, C).

(E) Number of progeny produced by *fog-2* females crossed to wild-type or *glna(−)* males.

(F) Numbers of non-Dpy and Dpy progeny produced by *dyp-10* hermaphrodites crossed to wild-type or *glna(−)* males. Data are represented as mean ± SD with individual values shown as dots in (B, C, E, F) and mean ± SD in (D). ns, p > 0.05; **, p < 0.01; ****, p < 0.0001 by two-tailed Student's *t* test. See also Figures S1−S3.

senescent cells. Targeted inhibition of GLS1 could become a new strategy for inducing senescent cell removal *in vivo*.[7]

In this study, we report the function of glutaminase in regulating sperm function. By generating a triple mutant that harbors a loss-of-function allele for each of all three mammalian glutaminase orthologs, we found that glutaminase gene activity is required for optimal *C. elegans* sperm function. Tissue-specific gene manipulations showed that germline glutaminase gene activity plays an important role. Moreover, transcriptional profiling analysis suggested a cellular redox imbalance in the glutaminase mutant and anti-oxidant treatment rescued the sperm defects in these animals. Our data indicate that glutaminase gene activity promotes sperm function by maintaining cellular redox homeostasis. As maintaining a low level of ROS is crucial to mammalian sperm function,[2] it is very likely that glutaminase plays a similar role in mammals.

RESULTS

Loss of mammalian glutaminase orthologs causes reduced fertility in *Caenorhabditis elegans*

We identified 3 genes, *glna-1*, *glna-2*, and *glna-3*, in the *C. elegans* genome that are orthologous to the mammalian *Gls1* and *Gls2* genes based on sequence homology (Figure S1). To understand the biological function of these *C. elegans* glutaminase orthologs, we generated a mutant for each gene using the CRISPR/Cas9 technique. The mutation includes a deletion with or without an additional single-nucleotide change. In all cases, a premature stop codon forms at the deletion site and the resulting truncated peptide lacks the entire highly conserved glutaminase catalytic domain (Figure 1A). We then crossed single mutants to generate double and triple mutants in case there is functional redundancy. All mutants did not show any

gross defect in somatic development (Figures S2A and S2C−S2E and data not shown). However, we observed changes in self-fertility brood size in these mutant hermaphrodites, with the most dramatic reduction seen in *glna-3; glna-2 glna-1* triple mutants (henceforth termed *glna(−)* for simplicity; 74.5% decrease relative to wild type; Figure 1B), although their reproductive span was not altered (Figure 1D). The *glna(−)* hermaphrodites also displayed a trend toward reduced lifespan (9.7% decrease relative to wild type; Figure S2B and Table S1).

C. elegans hermaphrodites lay unfertilized oocytes when self-sperm are depleted, because they only generate a set number of sperm during the last larval stage (L4) before switching to exclusive oocyte production.[8] While examining the self-fertility brood size of the *glna(−)* hermaphrodites, we noticed that unfertilized oocytes were also laid by these animals after their self-sperm had been depleted and that even though the timing of unfertilized oocyte production was similar between wild type and *glna(−)*, more unfertilized oocytes were laid by *glna(−)* hermaphrodites each day (Figure 1D). This dramatic increase in unfertilized oocytes (192.8% increase relative to wild type; Figure 1C) is suggestive of sperm deficiency in self-fertile *glna(−)* hermaphrodites. When mated, however, the brood size of a hermaphrodite is not limited by the number of self-sperm as extra sperm are provided by the male.[9] If the reduced self-fertility and concomitant increase in unfertilized oocytes in the *glna(−)* hermaphrodites are due to defects in their sperm, we would expect that provision of wild-type sperm through mating could rescue those phenotypes. Indeed, we observed an increase in their brood size and a reduction in unfertilized oocyte production in *glna(−)* hermaphrodites mated with wild-type males (Figures 1B and 1C), corroborating a deficiency in sperm number and/or activity in *glna(−)* hermaphrodites.

Nevertheless, we noticed that the brood size of *glna(−)* hermaphrodites mated with wild-type males was significantly smaller than that of wild-type hermaphrodites mated with wild-type males (Figure S3A), which would suggest a defect in oogenesis in *glna(−)* hermaphrodites. We, therefore, examined 1 day post-L4 (dpL4) *glna(−)* hermaphrodite germ lines using DIC microscopy and DAPI staining and found that the general patterning of the germ line appeared normal in these animals (Figure S3). We then quantified the number of germline progenitors in the distal proliferative zone and measured the proliferation rate of germline progenitors by calculating the mitotic index. We found that the level of germline proliferation was similar between wild-type and *glna(−)* hermaphrodites (Figures S3B−S3E). The level of germline apoptosis as determined by SYTO-12 staining was also comparable between the two groups (Figure S3F). Lastly, we measured the size of oocytes and found that *glna(−)* oocytes were smaller than their wild-type counterparts (Figures S3G−S3I). Although defective spermatogenesis could account for the reduced oocyte size of *glna(−)* hermaphrodites, as it has been reported that the sperm-derived major sperm protein (MSP) hormone drives oocyte growth by promoting actomyosin-dependent cytoplasmic streaming,[10,11] it is still possible that oogenesis is affected in the *glna(−)* hermaphrodites independent of their sperm defect. We decided to focus on the sperm defect in this study.

To test if *glna(−)* male sperm are generally defective in fertilization, we mated each wild-type or *glna(−)* male with one *fog-2* spermless female[12] and found that *glna(−)* males were able to produce as many progeny as wild-type males (Figure 1E). This result suggests that *glna(−)* male sperm are functional when competition against hermaphrodite sperm is not present. In wild type, however, male sperm outcompete hermaphrodite sperm when males and hermaphrodites are mated.[13] To further assess the ability of *glna(−)* male sperm to compete against hermaphrodite sperm, we mated wild-type or *glna(−)* males with *dyp-10* hermaphrodites at 1:1 ratio. *dyp-10* hermaphrodites were used to facilitate the separation of self-progeny (Dpy) from cross-progeny (non-Dpy). We found that the number of cross-progeny produced by *dyp-10* hermaphrodites mated with *glna(−)* males was comparable to the number of cross-progeny produced by those mated with wild-type males (Figure 1F), confirming a similar mating efficiency and sperm transfer for wild-type and *glna(−)* males. By contrast, significantly more self-progeny were produced by *dyp-10* hermaphrodites mated with *glna(−)* males (Figure 1F), indicating increased usage of self-sperm in those hermaphrodites. Together, these data suggest that even though *glna(−)* male sperm are competent for fertilization, their competitiveness against hermaphrodite sperm is compromised.

glna(+) is required for optimal sperm function

Next we characterized aspects of spermatogenesis that are crucial to sperm function in the *glna(−)* mutant. First, we quantified the number of spermatids in *glna(−)* hermaphrodites at 8 h post-L4 (hpL4) when spermatogenesis has completed and ovulation has just begun, so that we could have a relatively accurate
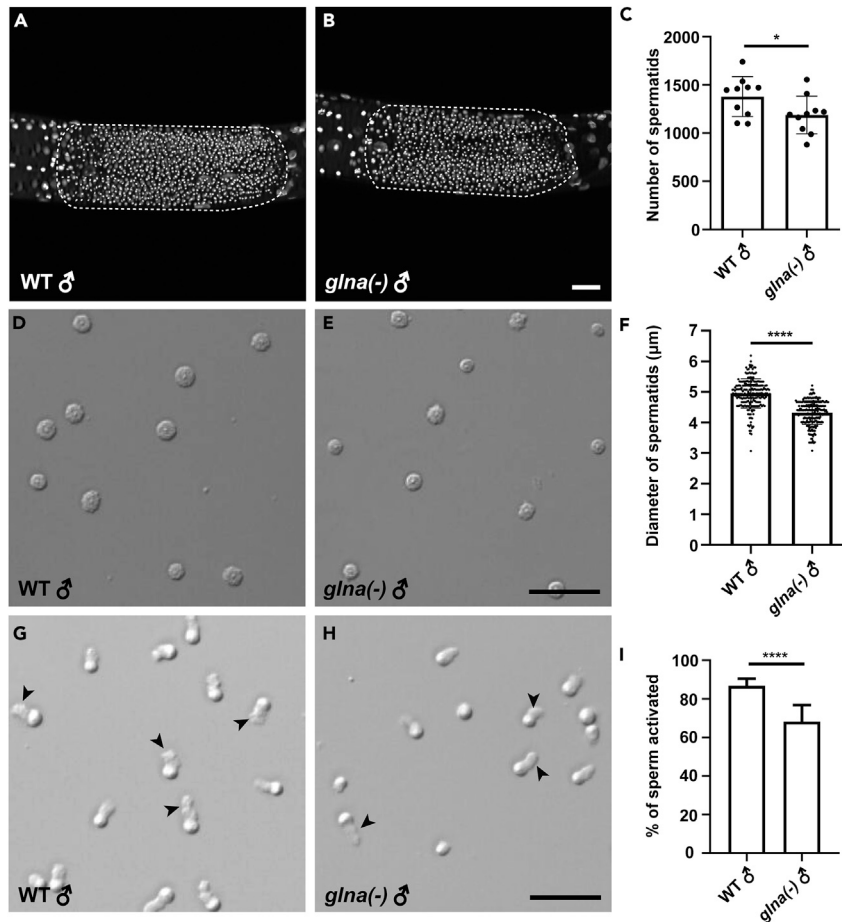
Figure 2. The *glna* genes regulate sperm function in *C. elegans*

(A and B) Representative DAPI-stained germ lines of 1 dpL4 wild-type and *glna(−)* virgin males. The dashed line outlines the spermatids.

(C) Number of spermatids in 1 dpL4 wild-type and *glna(−)* virgin males.

(D and E) Representative DIC images of spermatids isolated from 1 dpL4 wild-type and *glna(−)* males.

(F) Diameter of spermatids isolated from 1 dpL4 wild-type and *glna(−)* males.

(G and H) Representative DIC images of spermatids dissected from 1 dpL4 wild-type and *glna(−)* males after up to 30 min of pronase treatment. The arrowheads indicate the pseudopods.

(I) Percent of sperm from 1 dpL4 wild-type and *glna(−)* males activated by the pronase treatment. Scale bars: 20 μm. Data are represented as mean ± SD with individual values shown as dots in (C, F) and mean ± SD in (I). *, p < 0.05; ****, p < 0.0001 by two-tailed Student's *t* test in (C, F) and Fisher Exact test in (I). See also Figure S4.

measure of the total number of sperm produced in these animals. We found that *glna(−)* hermaphrodites had significantly fewer spermatids than those age-matched wild-type hermaphrodites (Figures S4A−S4C). Similarly, 1 dpL4 *glna(−)* virgin males had reduced number of spermatids compared with wild-type controls (Figures 2A−2C), suggesting that *glna(+)* is essential for generating the proper amount of sperm in both hermaphrodites and males. To account for the reduced number of spermatids in *glna(−)* males, we examined the levels of germline proliferation and apoptosis in these animals. In contrast to hermaphrodites (Figures S3B−S3E), the number of germline progenitors was reduced in 1 dpL4 *glna(−)* males relative to wild-type controls (Figures S4D−S4F). The proliferation rate of germline progenitors as evidenced by mitotic index, however, was elevated in *glna(−)* males (Figure S4G). We observed similar levels of germline apoptosis in wild-type and *glna(−)* males (Figure S4I), suggesting that apoptosis does not play a major role for the phenotype. Lastly, we found that *glna(−)* male germ lines had shorter distance to meiotic entry, indicating that reduced niche signaling could account for the smaller progenitor pool size in *glna(−)* males (Figure S4H).
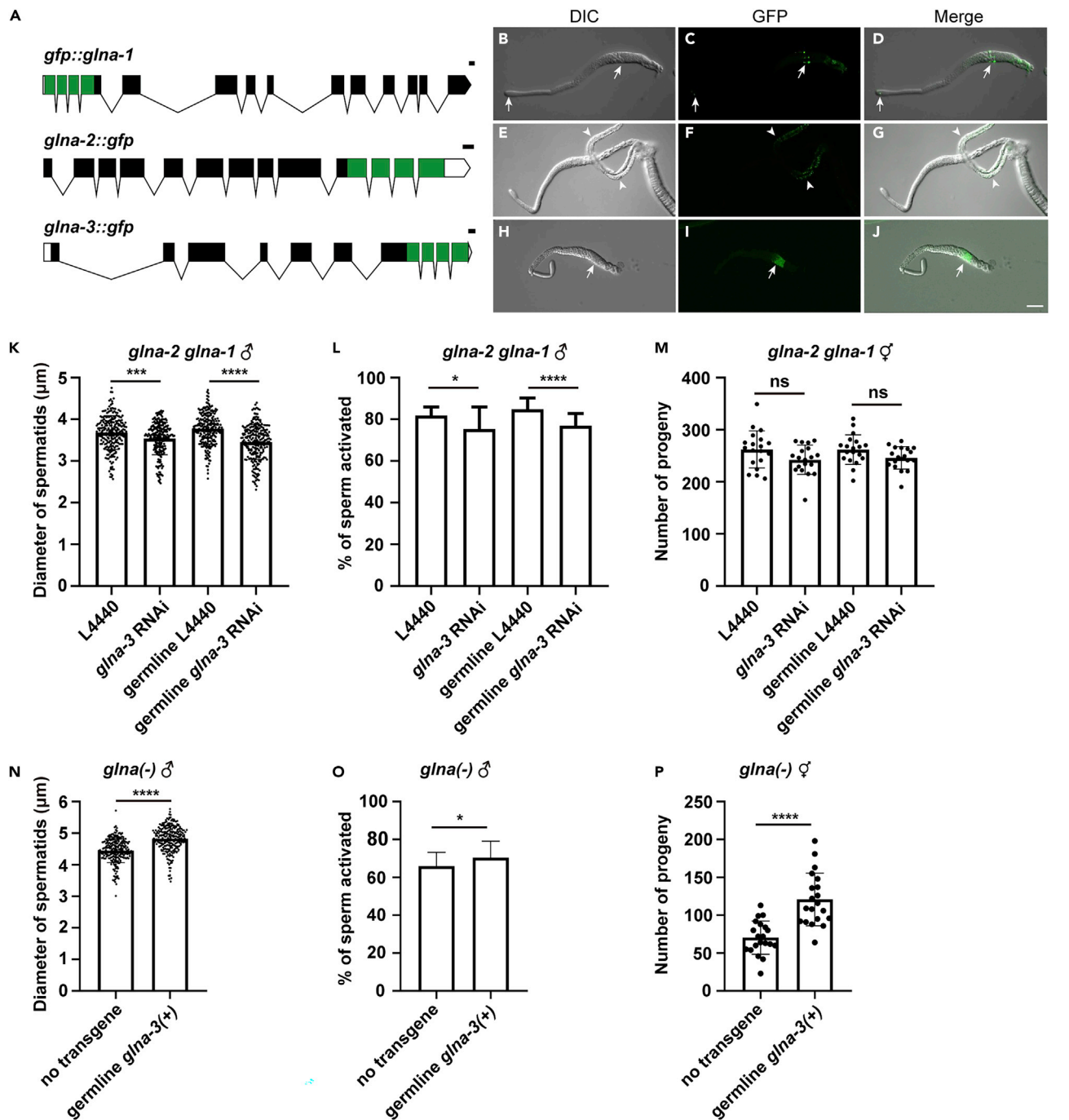
Figure 3. Germline *glna* gene activity is important for sperm function

(A) Schematics showing the *gfp*-tagged endogenous *glna-1*, *glna-2*, and *glna-3* loci. Solid boxes, exons; empty boxes, UTRs; lines, introns. The *gfp* sequence is highlighted in green. Scale bars, 100 bp.

(B–J) Germline expression of GLNA fusion proteins. All gonads are oriented distal end to the left. Scale bar: 50 μm. (B–D) Representative DIC (B), GFP (C), and merge (D) images of dissected gonads from 1 dpL4 *gfp::glna-1* males. GFP:GLNA-1 is expressed in the mitotic germline progenitors (left arrow) and developing spermatocytes (right arrow). (E–G) Representative DIC (E), GFP (F), and merge (G) images of dissected gonads from 1 dpL4 *glna-2::gfp* males. GLNA-2:GFP is undetectable in the germ line. Arrowheads indicate expression in the intestine. (H–J) Representative DIC (H), GFP (I), and merge (J) images of dissected gonads from 1 dpL4 *glna-3::gfp* males. GLNA-3:GFP is localized in the spermatids (arrow).

(K) Diameter of spermatids isolated from 1 dpL4 *glna-2 glna-1* and *rrf-1; glna-2 glna-1* males subject to control or *glna-3* RNAi.

(L) Percent of sperm from 1 dpL4 *glna-2 glna-1* and *rrf-1; glna-2 glna-1* males subject to control or *glna-3* RNAi activated by the pronase treatment.

(M) Number of progeny produced by self-fertile *glna-2 glna-1* and *rrf-1; glna-2 glna-1* hermaphrodites subject to control or *glna-3* RNAi.

Figure 3. Continued

(N) Diameter of spermatids isolated from 1 dpL4 *glna(−)* and *glna(−); Is(Pmex-5::glna-3(+)::nos-2 3'UTR)* males.

(O) Percent of sperm from 1 dpL4 *glna(−)* and *glna(−); Is(Pmex-5::glna-3(+)::nos-2 3'UTR)* males activated by the pronase treatment.

(P) Number of progeny produced by self-fertile *glna(−)* and *glna(−); Is(Pmex-5::glna-3(+)::nos-2 3'UTR)* hermaphrodites. Data are represented as mean ± SD with individual values shown as dots in (K, M, N, P) and mean ± SD in (L, O). ns, $p > 0.05$; *, $p < 0.05$; ***, $p < 0.001$; ****, $p < 0.0001$ by two-tailed Student's *t* test in (K, M, N, P) and Fisher Exact test in (L, O). See also Figure S5.

When comparing the number of sperm with the number of progeny produced by the *glna(−)* hermaphrodites (Figures S4A–S4C and 1B), we found a fertilization efficiency below 50%. This prompted us to examine additional functional properties of *glna(−)* sperm. We measured the size of spermatids isolated from 1 dpL4 *glna(−)* males and found that they were significantly smaller than those isolated from age-matched wild-type males (Figures 2D–2F). *C. elegans* spermatids acquire mobility through an activation process during which they form a pseudopod for crawling and this activation can be achieved *in vitro* by pronase or monensin treatment.[14,15] We first examined the response of spermatids dissected from 1 dpL4 wild-type or *glna(−)* males to pronase treatment. While over 80% of wild-type spermatids were fully activated after up to 30 min of pronase treatment (indicated by the presence of a fully extended pseudopod), *glna(−)* spermatids showed significantly lower levels of activation by the same treatment (Figures 2G–2I). Treatment with monensin confirmed a reduced activation rate for *glna(−)* spermatids (Figure S4J).

Together, these results suggest that loss of *glna* genes interferes with several aspects of *C. elegans* sperm development, which together contribute to the declined function of the *glna(−)* sperm.

Glna genes are expressed in the *Caenorhabditis elegans* male germ line

To determine the expression pattern of *C. elegans glna* genes, we generated GFP fusion proteins by using the CRISPR/Cas9 technique to insert a GFP-encoding sequence into the endogenous locus of *glna-1*, *glna-2*, and *glna-3*, respectively. Although C-terminal fusion proteins were desired to label as many isoforms as possible, we generated an N-terminal fusion protein for *glna-1* due to a potential off-target sgRNA binding site downstream of its C-terminus (Figure 3A). The three fusion proteins had distinct expression patterns in somatic tissues (Figure S5). Besides, we observed GFP fluorescence in the dissected 1 dpL4 male gonad of two reporter strains—GFP:GLNA-1 in the mitotic germline progenitors and developing spermatocytes (Figures 3B–3D) and GLNA-3:GFP in the spermatids (Figures 3H–3J), suggesting a functional role for both genes at different stages of spermatogenesis. Even though GFP fluorescence was not visible in the male gonad of the *glna-2* reporter strain, this does not preclude the possibility that *glna-2* is expressed at a very low level in some part of the male germ line (Figures 3E–3G).

Germline *glna(+)* is important for sperm function

Based on the expression pattern of *C. elegans glna* genes, we hypothesized that *glna(+)* acts germline-autonomously to promote sperm function. We first examined the germline requirement of *glna(+)* for optimal sperm function by tissue-specific RNAi. We tested the effect of knocking down *glna-3* in the *glna-2 glna-1* double mutant background in the presence or absence of *rrf-1*. Without *rrf-1*, RNAi effectiveness is reduced in the soma but retained in the germ line.[16,17] We found that knocking down *glna-3* by germline-directed RNAi resembled *glna-3* RNAi in the whole animal, both causing significant reduction in spermatid size and activation in 1 dpL4 *glna-2 glna-1* males (Figures 3K and 3L) and a trend toward reduced self-fertility brood size in *glna-2 glna-1* hermaphrodites (Figure 3M).

We then performed a tissue-specific rescue experiment in which we expressed wild-type *glna-3* cDNA in the germ line of *glna(−)* mutants by generating a single-copy insertion of the transgene *Pmex-5::glna-3::nos-2 3'UTR* using the CRISPR/Cas9 technique.[18,19] We chose *glna-3* because it has only one predicted isoform. Germline *glna-3* expression was able to increase spermatid size and activation of 1 dpL4 *glna(−)* males (Figures 3N and 3O) and restore self-fertility brood size of *glna(−)* hermaphrodites (Figure 3P). Therefore, we conclude that germline *glna(+)* is sufficient to improve sperm function in the *glna(−)* background.

Together, these data support the important role of germline *glna* gene activity in promoting *C. elegans* sperm function.
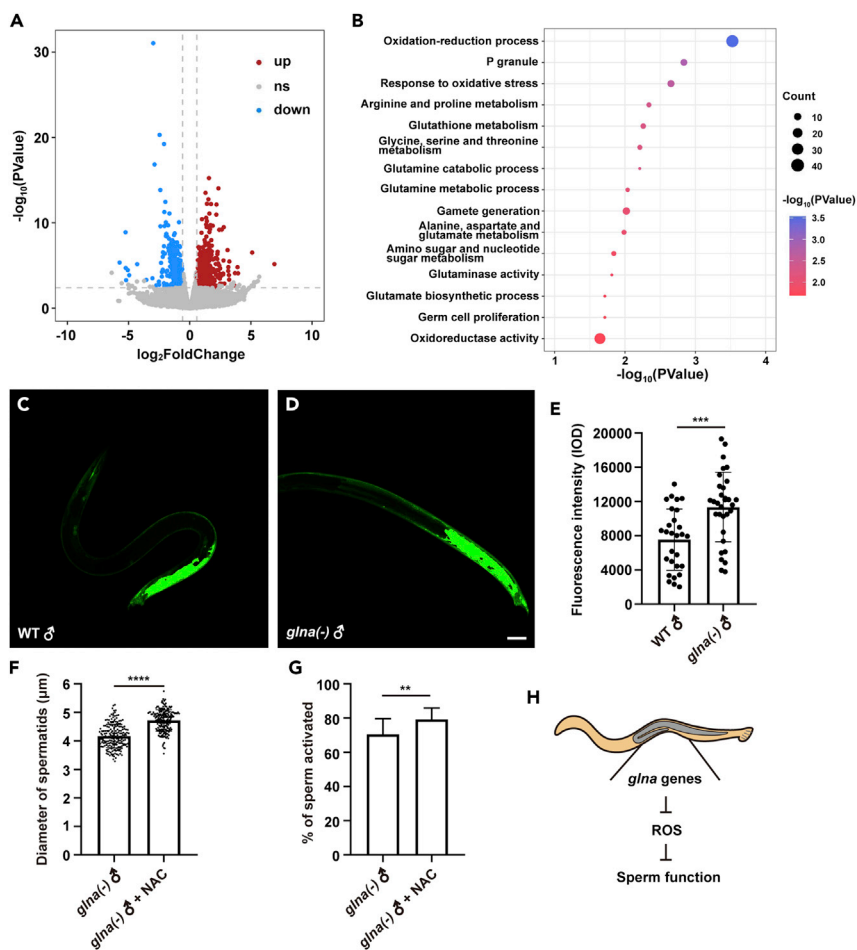
Figure 4. *C. elegans glna* genes promote sperm function by maintaining cellular redox homeostasis

(A) Volcano plot of genes obtained by RNA sequencing of L4 wild-type and *glna(−)* hermaphrodites. Red and blue dots represent genes up-regulated and down-regulated in *glna(−)*, respectively. Biological triplicates were used in this experiment.

(B) Statistical overrepresentation analysis of GO terms and KEGG pathways associated with our entire RNA-seq dataset using the DAVID functional annotation tool.

(C and D) Representative H_2DCFDA-stained 1 dpL4 wild-type and *glna(−)* males. Scale bar: 50 μm.

(E) Fluorescence intensity of H_2DCFDA-stained 1 dpL4 wild-type and *glna(−)* males.

(F) Diameter of spermatids isolated from 1 dpL4 *glna(−)* males with or without 2 mM NAC supplementation in their diet.

(G) Percent of sperm from 1 dpL4 *glna(−)* males with or without 2 mM dietary NAC supplementation activated by the pronase treatment. Data are represented as mean ± SD with individual values shown as dots in (E, F) and mean ± SD in (G). **, $p < 0.01$; ***, $p < 0.001$; ****, $p < 0.0001$ by two-tailed Student's t test in (E and F) and Fisher Exact test in (G).

(H) Model. The male germ line is shaded in gray. See also Figure S6 and Table S2.

Transcriptional profiling reveals a shift in redox homeostasis in *glna(−)*

To understand the mechanisms by which *glna(+)* promotes sperm function, we performed an RNA-seq experiment to compare the expression profiles of wild-type and *glna(−)* hermaphrodites at the L4 stage when spermatogenesis occurs. We identified a total of 1090 differentially expressed genes, among which 534 were up-regulated and 556 were down-regulated in *glna(−)* (fold change>1.5, FDR<0.05; Figure 4A). The complete dataset is available in Table S2.

To get an overview of the associated functional categories and pathways of our entire dataset, we performed Gene Ontology (GO) enrichment analysis and KEGG pathway analysis on all up- and down-regulated genes using the DAVID functional annotation tool (https://david.ncifcrf.gov).[20,21] As expected, GO terms associated with glutamine/glutamate metabolism were overrepresented (Figure 4B). Additional

highly enriched gene classes included those involved in the metabolism of several other amino acids such as proline, glycine, serine, alanine, and aspartate, consistent with a central role for glutamate in the biosynthesis of these non-essential amino acids (Figure 4B). Combined, these findings suggest that *C. elegans glna* genes encode functional glutaminases.

In line with the phenotypic outcome of disrupting all *C. elegans glna* genes, we also observed significant enrichment of the GO terms "gamete generation," "germ cell proliferation," and "P granule" in our analysis (Figure 4B). Specifically, many genes in the MSP family which comprises ~15% of protein content in the *C. elegans* sperm and mediates their motility[22] were down-regulated in *glna(−)* (Table S2). This down-regulation of MSPs could account for the reduced oocyte size observed in the *glna(−)* hermaphrodites as discussed above (Figures S3G–S3I).

Among the most significantly overrepresented gene groups were "oxidation-reduction process," "oxidoreductase activity," "response to oxidative stress," and "glutathione metabolism" (Figure 4B). Glutathione is a tripeptide composed of glutamate, cysteine, and glycine. The conversion of glutamine to glutamate by glutaminase is key to glutathione synthesis because glutamate levels also control the availability of the other two amino acid components of glutathione. Importantly, glutathione is a major cellular antioxidant that neutralizes reactive oxygen species (ROS).[6] The identification of these gene classes highlights a change in the cellular redox state of the *glna(−)* mutant and a metabolic adaptation in these animals to maintain redox homeostasis.

glna(+) promotes sperm function by maintaining cellular redox homeostasis

Although low levels of ROS are required for successful sperm capacitation and hyperactivation in mammals, excessive ROS is detrimental to sperm function through mechanisms such as lipid peroxidation and DNA damage.[2] Recently, studies in *C. elegans* showed that ROS drives sperm defects in mutants with incomplete proline catabolism.[23,24] Since our RNA-seq results suggested a cellular redox imbalance in *glna(−)*, we reasoned that the level of ROS may have increased in these animals. We stained 1 dpL4 *glna(−)* hermaphrodites and males with 2′,7′-dichlorofluorescein diacetate (H$_2$DCFDA), a commonly used fluorescent probe for *in vivo* detection of intracellular ROS levels[25] and found that both *glna(−)* hermaphrodites and males exhibited higher levels of ROS compared with wild-type controls (Figures S6A–S6C and 4C–4E, respectively).

If it is the increase of cellular ROS that causes the sperm defects in *glna(−)*, then supplementing the diet of *glna(−)* animals with antioxidants should alleviate those phenotypes. Dietary N-acetylcysteine (NAC) supplementation has been used as an effective way to reduce ROS levels in *C. elegans*.[24,26] Indeed, 2 mM NAC supplementation significantly restored both spermatid size and activation of 1 dpL4 *glna(−)* males (Figures 4F, 4G, and S6D) and improved *glna(−)* male sperm competitiveness against hermaphrodite sperm (Figure S6E). In addition, we found that germline *glna-3* expression was able to suppress the increased ROS staining in *glna(−)* animals (Figure S6F). Together, these results indicate that *glna(+)* promotes sperm function by maintaining cellular redox homeostasis.

DISCUSSION

Our data show that the *C. elegans* glutaminase orthologs support proper sperm function likely in the germ line by maintaining cellular redox homeostasis (Figure 4H). Here we use the term "sperm function" to refer to aspects of spermatogenesis that are key to sperm function rather than those biological processes involved in fertilization such as the recognition, adhesion, and fusion of the sperm with the oocyte. This result has two major implications.

First, we have discovered a regulator of sperm function. Mitochondrial glutaminase activity controls cellular redox balance and its inhibition is linked to elevated ROS levels in cancer cells.[27] Besides, ROS-mediated damage to spermatozoa contributes to a significant portion of human male infertility, and maintaining a low level of ROS is essential to human sperm function.[2] Therefore, it is very likely that this role of glutaminase in regulating sperm function is conserved in mammals. Although mammalian studies are still needed to confirm this idea, some indirect evidence suggest that it would be the case. In particular, the tumor-suppressor gene *P53*, which is expressed in the mammalian primary spermatocytes, plays an important part in spermatogenesis during the prophase of meiosis. This role of *P53* may be linked to its function in the upregulation of many antioxidant genes including *Gls2*.[28]

Second, our finding highlights the utility of *C. elegans* as a tool for discovering genes that regulate sperm function. Despite the many differences between *C. elegans* and mammalian male germ cell development, common features are shared by both systems especially during the process when spermatozoa become fertilization-competent. As a result, *C. elegans* has been used as a model for understanding the cell biology and genetics of spermatogenesis. Genetic screens have been carried out in *C. elegans* to identify factors that regulate sperm function. So far ~60 *spe* (sperm-defective) mutants have been isolated and many of the affected genes have been identified.[15,29–33] Besides our analysis, several previous studies have shown that endogenous ROS level is crucial to optimal sperm activity in *C. elegans*. For instance, genes involved in proline catabolism affect *C. elegans* sperm function and male reproductive advantage and they do so by controlling cellular ROS level and mitochondrial dynamics.[23,24] We speculate that other cellular requirements may also be shared between *C. elegans* and mammalian sperm in order to achieve reproductive success. Therefore, we propose to take advantage of the ample genetic tools available in *C. elegans* to identify additional factors that regulate sperm function, and evolutionarily conserved mechanisms will likely be uncovered.

In our analysis, we noticed a difference in *glna* activity to regulate *C. elegans* hermaphrodite and male sperm function: while *glna(−)* hermaphrodite sperm are dysfunctional in self-fertilization, *glna(−)* male sperm are functional when competition against hermaphrodite sperm is absent, and only lose their superiority in their competition against hermaphrodite sperm. Since hermaphrodite sperm rely on a single activation pathway (*spe-8*) while male sperm can be activated by either of two redundant pathways (*spe-8* and *try-5*),[34] it is possible that only activation through the *spe-8* pathway is affected in the *glna(−)* mutant, so that although the self-fertility of *glna(−)* hermaphrodites was greatly reduced, a decrease in *glna(−)* male fertility was not observed when competition against hermaphrodite sperm is not required. We will test this hypothesis in our future analysis.

Recently, the mammalian *Gls1* gene has been implicated in cellular senescence.[7] Except for its influence on the sperm of young animals, glutaminase may also affect the age-associated decline of sperm function. Since postponing childbearing to advanced age is a major cause of decreased human sperm quality and hence infertility, it would be interesting to investigate if glutaminase gene activity maintains sperm function over time.

Limitations of the study

Our data suggest that oocyte production may be affected in the *glna(−)* mutant, even though both germline proliferation and apoptosis were not altered in the oogenic *glna(−)* germ line. While we focused the current analysis on the sperm defect of the *glna(−)* animals, whether oogenesis is independently affected by the *glna* mutations and by which mechanisms glutaminase gene activity regulates oocyte production need to be further addressed.

STAR★METHODS

Detailed methods are provided in the online version of this paper and include the following:

- KEY RESOURCES TABLE
- RESOURCE AVAILABILITY
  - Lead contact
  - Materials availability
  - Data and code availability
- EXPERIMENTAL MODEL AND SUBJECT DETAILS
  - *C. elegans* strains and maintenance
- METHOD DETAILS
  - Protein sequence alignment
  - Generation of *C. elegans* strains
  - Developmental timing
  - Body length
  - Fertility
  - Lifespan
  - Analysis of germline progenitor cells
  - Apoptosis

- ○ Oocyte size
- ○ Sperm number
- ○ Sperm size
- ○ Sperm activation with pronase and monensin
- ○ GFP microscopy of GLNA fusion proteins
- ○ RNAi
- ○ RNA-seq
- ○ Measurement of ROS
- ○ NAC supplementation
- ● QUANTIFICATION AND STATISTICAL ANALYSIS

SUPPLEMENTAL INFORMATION

Supplemental information can be found online at https://doi.org/10.1016/j.isci.2023.106206.

AUTHOR CONTRIBUTIONS

Conceptualization, Z.Q. and J.C.Z.; Methodology, Z.Q.; Investigation, Q.L., H.Y., and Z.Z.; Writing - Original Draft, Z.Q. and Q.L.; Writing - Review & Editing, Z.Q. and Q.L.; Funding Acquisition, Z.Q. and J.C.Z.; Resources, Z.Q.; Supervision, Z.Q. and J.C.Z.

DECLARATION OF INTERESTS

The authors declare no competing interests.

REFERENCES

1. Dai, C., Zhang, Z., Shan, G., Chu, L.T., Huang, Z., Moskovtsev, S., Librach, C., Jarvi, K., and Sun, Y. (2021). Advances in sperm analysis: techniques, discoveries and applications. Nat. Rev. Urol. *18*, 447–467. https://doi.org/10.1038/s41585-021-00472-2.

2. Bisht, S., Faiq, M., Tolahunase, M., and Dada, R. (2017). Oxidative stress and male infertility. Nat. Rev. Urol. *14*, 470–485. https://doi.org/10.1038/nrurol.2017.69.

3. Nishimura, H., and L'Hernault, S.W. (2017). Spermatogenesis. Curr. Biol. *27*, R988–R994. https://doi.org/10.1016/j.cub.2017.07.067.

4. Masisi, B.K., El Ansari, R., Alfarsi, L., Rakha, E.A., Green, A.R., and Craze, M.L. (2020). The role of glutaminase in cancer. Histopathology *76*, 498–508. https://doi.org/10.1111/his.14014.

5. Ding, L., Xu, X., Li, C., Wang, Y., Xia, X., and Zheng, J.C. (2021). Glutaminase in microglia: a novel regulator of neuroinflammation. Brain Behav. Immun. *92*, 139–156. https://doi.org/10.1016/j.bbi.2020.11.038.

6. Altman, B.J., Stine, Z.E., and Dang, C.V. (2016). From Krebs to clinic: glutamine metabolism to cancer therapy. Nat. Rev. Cancer *16*, 619–634. https://doi.org/10.1038/nrc.2016.71.

7. Johmura, Y., Yamanaka, T., Omori, S., Wang, T.W., Sugiura, Y., Matsumoto, M., Suzuki, N., Kumamoto, S., Yamaguchi, K., Hatakeyama, S., et al. (2021). Senolysis by glutaminolysis inhibition ameliorates various age-associated disorders. Science *371*, 265–270. https://doi.org/10.1126/science.abb5916.

8. Zanetti, S., and Puoti, A. (2013). Sex determination in the Caenorhabditis elegans germline. Adv. Exp. Med. Biol. *757*, 41–69. https://doi.org/10.1007/978-1-4614-4015-4_3.

9. Marcello, M.R., Singaravelu, G., and Singson, A. (2013). Fertilization. Adv. Exp. Med. Biol. *757*, 321–350. https://doi.org/10.1007/978-1-4614-4015-4_11.

10. Govindan, J.A., Nadarajan, S., Kim, S., Starich, T.A., and Greenstein, D. (2009). Somatic cAMP signaling regulates MSP-dependent oocyte growth and meiotic maturation in C. elegans. Development *136*, 2211–2221. https://doi.org/10.1242/dev.034595.

11. Nadarajan, S., Govindan, J.A., McGovern, M., Hubbard, E.J.A., and Greenstein, D. (2009). MSP and GLP-1/Notch signaling coordinately regulate actomyosin-dependent cytoplasmic streaming and oocyte growth in C. elegans. Development *136*, 2223–2234. https://doi.org/10.1242/dev.034603.

12. Schedl, T., and Kimble, J. (1988). fog-2, a germ-line-specific sex determination gene required for hermaphrodite spermatogenesis in Caenorhabditis elegans. Genetics *119*, 43–61. https://doi.org/10.1093/genetics/119.1.43.

13. LaMunyon, C.W., and Ward, S. (1995). Sperm precedence in a hermaphroditic nematode (Caenorhabditis elegans) is due to competitive superiority of male sperm. Experientia 51, 817–823. https://doi.org/10.1007/BF01922436.

14. Shakes, D.C., and Ward, S. (1989). Initiation of spermiogenesis in C. elegans: a pharmacological and genetic analysis. Dev. Biol. 134, 189–200. https://doi.org/10.1016/0012-1606(89)90088-2.

15. Shakes, D.C., and Ward, S. (1989). Mutations that disrupt the morphogenesis and localization of a sperm-specific organelle in Caenorhabditis elegans. Dev. Biol. 134, 307–316. https://doi.org/10.1016/0012-1606(89)90103-6.

16. Sijen, T., Fleenor, J., Simmer, F., Thijssen, K.L., Parrish, S., Timmons, L., Plasterk, R.H., and Fire, A. (2001). On the role of RNA amplification in dsRNA-triggered gene silencing. Cell 107, 465–476. https://doi.org/10.1016/s0092-8674(01)00576-1.

17. Kumsta, C., and Hansen, M. (2012). C. elegans rrf-1 mutations maintain RNAi efficiency in the soma in addition to the germline. PLoS One 7, e35428. https://doi.org/10.1371/journal.pone.0035428.

18. D'Agostino, I., Merritt, C., Chen, P.L., Seydoux, G., and Subramaniam, K. (2006). Translational repression restricts expression of the C. elegans Nanos homolog NOS-2 to the embryonic germline. Dev. Biol. 292, 244–252. https://doi.org/10.1016/j.ydbio.2005.11.046.

19. Merritt, C., Rasoloson, D., Ko, D., and Seydoux, G. (2008). 3' UTRs are the primary regulators of gene expression in the C. elegans germline. Curr. Biol. 18, 1476–1482. https://doi.org/10.1016/j.cub.2008.08.013.

20. Huang, D.W., Sherman, B.T., and Lempicki, R.A. (2009). Systematic and integrative analysis of large gene lists using DAVID bioinformatics resources. Nat. Protoc. 4, 44–57. https://doi.org/10.1038/nprot.2008.211.

21. Huang, D.W., Sherman, B.T., and Lempicki, R.A. (2009). Bioinformatics enrichment tools: paths toward the comprehensive functional analysis of large gene lists. Nucleic Acids Res. 37, 1–13. https://doi.org/10.1093/nar/gkn923.

22. Klass, M.R., and Hirsh, D. (1981). Sperm isolation and biochemical analysis of the major sperm protein from Caenorhabditis elegans. Dev. Biol. 84, 299–312. https://doi.org/10.1016/0012-1606(81)90398-5.

23. Yen, C.A., Ruter, D.L., Turner, C.D., Pang, S., and Curran, S.P. (2020). Loss of flavin adenine dinucleotide (FAD) impairs sperm function and male reproductive advantage in C. elegans. Elife 9, e52899. https://doi.org/10.7554/eLife.52899.

24. Yen, C.A., and Curran, S.P. (2021). Incomplete proline catabolism drives premature sperm aging. Aging Cell 20, e13308. https://doi.org/10.1111/acel.13308.

25. Schulz, T.J., Zarse, K., Voigt, A., Urban, N., Birringer, M., and Ristow, M. (2007). Glucose restriction extends Caenorhabditis elegans life span by inducing mitochondrial respiration and increasing oxidative stress. Cell Metab. 6, 280–293. https://doi.org/10.1016/j.cmet.2007.08.011.

26. Desjardins, D., Cacho-Valadez, B., Liu, J.L., Wang, Y., Yee, C., Bernard, K., Khaki, A., Breton, L., and Hekimi, S. (2017). Antioxidants reveal an inverted U-shaped dose-response relationship between reactive oxygen species levels and the rate of aging in Caenorhabditis elegans. Aging Cell 16, 104–112. https://doi.org/10.1111/acel.12528.

27. Boese, A.C., and Kang, S. (2021). Mitochondrial metabolism-mediated redox regulation in cancer progression. Redox Biol. 42, 101870. https://doi.org/10.1016/j.redox.2021.101870.

28. Hu, W., Zhang, C., Wu, R., Sun, Y., Levine, A., and Feng, Z. (2010). Glutaminase 2, a novel p53 target gene regulating energy metabolism and antioxidant function. Proc. Natl. Acad. Sci. USA 107, 7455–7460. https://doi.org/10.1073/pnas.1001006107.

29. L'Hernault, S.W., Shakes, D.C., and Ward, S. (1988). Developmental genetics of chromosome I spermatogenesis-defective mutants in the nematode Caenorhabditis elegans. Genetics 120, 435–452. https://doi.org/10.1093/genetics/120.2.435.

30. Minniti, A.N., Sadler, C., and Ward, S. (1996). Genetic and molecular analysis of spe-27, a gene required for spermiogenesis in Caenorhabditis elegans hermaphrodites. Genetics 143, 213–223. https://doi.org/10.1093/genetics/143.1.213.

31. Nance, J., Minniti, A.N., Sadler, C., and Ward, S. (1999). spe-12 encodes a sperm cell surface protein that promotes spermiogenesis in Caenorhabditis elegans. Genetics 152, 209–220. https://doi.org/10.1093/genetics/152.1.209.

32. Nance, J., Davis, E.B., and Ward, S. (2000). spe-29 encodes a small predicted membrane protein required for the initiation of sperm activation in Caenorhabditis elegans.

Genetics 156, 1623–1633. https://doi.org/10.1093/genetics/156.4.1623.

33. Geldziler, B., Chatterjee, I., and Singson, A. (2005). The genetic and molecular analysis of spe-19, a gene required for sperm activation in Caenorhabditis elegans. Dev. Biol. 283, 424–436. https://doi.org/10.1016/j.ydbio.2005.04.036.

34. Chu, D.S., and Shakes, D.C. (2013). Spermatogenesis. Adv. Exp. Med. Biol. 757, 171–203. https://doi.org/10.1007/978-1-4614-4015-4_7.

35. Brenner, S. (1974). The genetics of Caenorhabditis elegans. Genetics 77, 71–94. https://doi.org/10.1093/genetics/77.1.71.

36. Qin, Z., and Hubbard, E.J.A. (2015). Non-autonomous DAF-16/FOXO activity antagonizes age-related loss of C. elegans germline stem/progenitor cells. Nat. Commun. 6, 7107. https://doi.org/10.1038/ncomms8107.

37. Michaelson, D., Korta, D.Z., Capua, Y., and Hubbard, E.J.A. (2010). Insulin signaling promotes germline proliferation in C. elegans. Development 137, 671–680. https://doi.org/10.1242/dev.042523.

38. Achache, H., Falk, R., Lerner, N., Beatus, T., and Tzur, Y.B. (2021). Oocyte aging is controlled by mitogen-activated protein kinase signaling. Aging Cell 20, e13386. https://doi.org/10.1111/acel.13386.

39. Zhao, Y., Tan, C.H., Krauchunas, A., Scharf, A., Dietrich, N., Warnhoff, K., Yuan, Z., Druzhinina, M., Gu, S.G., Miao, L., et al. (2018). The zinc transporter ZIPT-7.1 regulates sperm activation in nematodes. PLoS Biol. 16, e2005069. https://doi.org/10.1371/journal.pbio.2005069.

40. Timmons, L., Court, D.L., and Fire, A. (2001). Ingestion of bacterially expressed dsRNAs can produce specific and potent genetic interference in Caenorhabditis elegans. Gene 263, 103–112. https://doi.org/10.1016/S0378-1119(00)00579-5.

41. Yang, Z.Z., Yu, Y.T., Lin, H.R., Liao, D.C., Cui, X.H., and Wang, H.B. (2018). Lonicera japonica extends lifespan and healthspan in Caenorhabditis elegans. Free Radic. Biol. Med. 129, 310–322. https://doi.org/10.1016/j.freeradbiomed.2018.09.035.

42. Yoon, D.S., Lee, M.H., and Cha, D.S. (2018). Measurement of intracellular ROS in Caenorhabditis elegans using 2',7'-dichlorodihydrofluorescein diacetate. Bio. Protoc. 8, e2774. https://doi.org/10.21769/BioProtoc.2774.

STAR★METHODS

KEY RESOURCES TABLE

REAGENT or RESOURCE	SOURCE	IDENTIFIER
Bacterial and virus strains		
Escherichia coli: OP50	Caenorhabditis Genetics Center	WormBase ID: OP50
Escherichia coli: HT115	Caenorhabditis Genetics Center	WormBase ID: HT115(DE3)
Chemicals, peptides, and recombinant proteins		
Pronase E	Sigma	D8811
Monensin	Invitrogen	00-4505-51
VECTASHIELD mounting medium with DAPI	Vector Laboratories	H-1200
SYTO-12	Invitrogen	S7574
Trizol	Ambion	15596026
Chloroform	SINOPHARM	10006818
Isopropanol	SINOPHARM	80109218
2′,7′-dichlorofluorescein diacetate	Sigma	D6883
N-acetylcysteine	Solarbio	C8460
Critical commercial assays		
Seamless Cloning Kit	Beyotime	D7010s
Deposited data		
RNA-seq data	This paper	GEO: GSE224117
Experimental models: Organisms/strains		
C. elegans: N2: *C. elegans*, Bristol isolate	Caenorhabditis Genetics Center	WB Strain: N2
C. elegans: PHX1405: *glna-1(syb1405)*	SunyBiotech	N/A
C. elegans: PHX1406: *glna-2(syb1406)*	SunyBiotech	N/A
C. elegans: PHX1403: *glna-3(syb1403)*	SunyBiotech	N/A
C. elegans: QIN21: *glna-2(syb1406) glna-1(syb1405)*	This paper	N/A
C. elegans: QIN22: *glna-3(syb1403); glna-1(syb1405)*	This paper	N/A
C. elegans: QIN23: *glna-3(syb1403); glna-2(syb1406)*	This paper	N/A
C. elegans: QIN24: *glna-3(syb1403); glna-2(syb1406) glna-1(syb1405)*	This paper	N/A
C. elegans: BS553: *fog-2(oz40)*	Caenorhabditis Genetics Center	WB Strain: BS553
C. elegans: FDU329: *dpy-10(shc5)*	Zhiyong Shao	N/A
C. elegans: PHX4148: *gfp::glna-1*	SunyBiotech	N/A
C. elegans: PHX4077: *glna-2::gfp*	SunyBiotech	N/A
C. elegans: PHX3987: *glna-3::gfp*	SunyBiotech	N/A
C. elegans: QIN49: *rrf-1(pk1417); glna-2(syb1406) glna-1(syb1405)*	This paper	N/A
C. elegans: QIN81: *glna-3(syb1403); glna-2(syb1406) glna-1(syb1405); sybIs6816(Pmex-5::glna-3::nos-2 3′-UTR)*	This paper	N/A
Recombinant DNA		
Plasmid: *Pmex-5::glna-3::nos-2 3′UTR*	This paper	N/A
Plasmid: *glna-3* RNAi	This paper	N/A
Software and algorithms		
ClustalX	Clustal	www.clustal.org
Jalview	Jalview	www.jalview.org/getdown/release/

(Continued on next page)

Continued

REAGENT or RESOURCE	SOURCE	IDENTIFIER
Zeiss Zen Imaging Software	Zeiss	https://www.zeiss.com/microscopy/int/products/microscope-software/zen.html
ImageJ	NIH	https://imagej.nih.gov/ij/
DAVID	LHRI	https://david.ncifcrf.gov
GraphPad Prism 8	GraphPad	https://www.graphpad.com/scientific-software/prism/
Adobe Illustrator CS5	Adobe	https://www.adobe.com/products/illustrator.html

RESOURCE AVAILABILITY

Lead contact

Further information and requests for resources and reagents should be directed to and will be fulfilled by the lead contact, Zhao Qin (zqin.med@tongji.edu.cn).

Materials availability

All *C. elegans* strains and plasmids generated in this study are available on request from the lead contact.

Data and code availability

- RNA-seq data have been deposited at GEO and are publicly available as of the date of publication. The accession number is listed in the key resources table. Other data reported in this paper will be shared by the lead contact upon request.

- This paper does not report original code.

- Any additional information required to reanalyze the data reported in this paper is available from the lead contact upon request.

EXPERIMENTAL MODEL AND SUBJECT DETAILS

C. elegans strains and maintenance

Strains were derived from N2 wild type (Bristol) and handled using standard methods.[35] Unless otherwise indicated, worms were grown on OP50 at 20°C. All strains used in this study are listed in the key resources table.

METHOD DETAILS

Protein sequence alignment

The following protein sequences are aligned in Figure S1, identified by species, isoform, and NCBI reference sequence code: CeGLNA-1 (*C. elegans*, isoform a, NP_497054.2), CeGLNA-2 (*C. elegans*, isoform a, NP_495675.1), CeGLNA-3 (*C. elegans*, NP_492162.1), MmGls1 (*Mus musculus*, mitochondrial isoform 1, NP_001074550.1), MmGls2 (*M. musculus*, mitochondrial isoform 1, NP_001028436.2), HsGLS1 (*Homo sapiens*, isoform 1 precursor, NP_055720.3), and HsGLS2 (*H. sapiens*, isoform 1 precursor, NP_037399.2). The alignment was performed using ClustalX.

Generation of *C. elegans* strains

The *glna* mutant alleles, *gfp* knock-in animals, and germline *glna-3*-expressing transgene were generated at SunyBiotech (Suzhou, China). To generate the germline *glna-3*-expressing transgene, a 488 bp *mex-5* promoter, a *glna-3*-encoding sequence amplified from N2 cDNA, and a 433 bp *nos-2 3'UTR* were placed together by Gibson assembly (Seamless Cloning Kit, Beyotime). Double and triple mutants of *glna* genes and germline *glna-3*-expressing *glna(−)* animals were then obtained by standard crossing procedure.

Developmental timing

50 gravid adults were transferred to 5 freshly seeded NGM plates (10 worms per plate), allowed to lay eggs for 2 h, and then removed. The total number of worms and the number of L4 larvae on each plate were counted every 2 h from 44 to 52 h post egg-laying. Fraction of L4 worms was calculated.

Body length

Worms were transferred onto NGM plates at the L4 stage. 24 h later, they were washed off the plates with M9 buffer, anesthetized in 20 mM levamisole in M9, and placed on a 4% agarose pad without coverslip. They were then aligned with a hair pick and visualized under a Zeiss Imager M1 (Carl Zeiss) using DIC optics. Their body length was measured using the ImageJ software.

Fertility

To measure hermaphrodite self-fertility, individual L4 hermaphrodites were placed on fresh NGM plates and transferred onto new plates every 24 h until egg-laying ceased. The number of unfertilized oocytes and the number of progeny on each plate were scored 24 and 48 h after the hermaphrodite was removed from the plate, respectively.

To measure mated fertility, individual L4 hermaphrodites were each crossed to one young adult male for 24 h. Then the males were removed and the hermaphrodites were transferred to new NGM plates every 24 h until egg-laying ceased. The success of mating was confirmed by the presence of male progeny and the numbers of progeny and unfertilized oocytes were counted at the same time points as described above. For the sperm competition experiment, offspring were scored as Dpy (self-progeny) or non-Dpy (cross-progeny) upon reaching adulthood.

Lifespan

~100 L4 (t0) larvae were picked and transferred onto fresh plates every other day until reproduction cessation. Their survival status was recorded until all the animals died. Worms that crawled off the plate or died as a result of extruded internal organs ("bursting") or internally hatched progeny ("bagging") were censored but were included in the statistical analysis as censored animals. Survival curves were generated using GraphPad Prism and analyzed using Mantel-Cox log rank test.[36]

Analysis of germline progenitor cells

Worms were washed off plates with M9 buffer, fixed in 100% ethanol for 5 min, and stained using VECTASHIELD mounting medium with DAPI (Vector Laboratories). z stack images of the distal germ line were acquired with a Zeiss Imager M1 equipped with an Apotome Axioimager (Carl Zeiss). The number of germline progenitors included all the germ cells between the distal tip and the beginning of meiotic entry, defined as the first row of cells in which two or more nuclei displayed the characteristic crescent shape. The mitotic index was determined as the percentage of metaphase and anaphase figures over the total number of proliferative zone nuclei and distance to meiotic entry was measured in cell diameters from the distal tip to the meiotic entry border.[36]

Apoptosis

The number of apoptotic corpses in the germ line was estimated using the vital dye SYTO-12 (Invitrogen): worms were washed in M9, incubated in 200 μL of 33 μM SYTO-12 in M9 for 5 h at room temperature in the dark, destained for 1 h in the dark on an NGM plate freshly seeded with OP50, and scored live while paralyzed in levamisole.[37]

Oocyte size

Synchronized 1 dpL4 hermaphrodites were mounted in M9 and visualized under a Zeiss Imager M1 using DIC optics.[38] Mid-oocyte plane areas of −1, −2, and −3 oocytes were measured using the ImageJ software.

Sperm number

Ethanol fixation and DAPI staining were performed as described above. Worms were then imaged under a Zeiss Imager M1 equipped with an Apotome Axioimager and z stack images of the proximal germ line were acquired. Spermatids were recognized by their characteristic nuclear stain and the number of spermatids was counted through all planes of the z stack using the ImageJ software.

Sperm size

Synchronized 1 dpL4 males were dissected in 20 μL SM buffer (50 mM HEPES, 45 mM NaCl, 25 mM KCl, 1 mM MgCl$_2$, 5 mM CaCl$_2$, 10 mg/mL PVP) to release spermatids. Released spermatids were immediately

imaged under a Zeiss Imager M1 and DIC images were captured. The diameter of the spherical spermatids was measured using the ImageJ software.[23,24]

Sperm activation with pronase and monensin

Synchronized 1 dpL4 males were dissected in 20 μL SM buffer supplemented with 200 μg/mL pronase E (Sigma) or 250 nM monensin (Invitrogen). Released spermatids were incubated at room temperature for up to 30 min, and imaged under a Zeiss Imager M1 using DIC optics. The total number of sperm and the number of activated sperm (determined by the presence of a fully extended pseudopod) were counted using the ImageJ software and the percentage of activated sperm was calculated.[39]

GFP microscopy of GLNA fusion proteins

Synchronized whole worms and freshly dissected gonads were imaged under a Zeiss Imager M1 using DIC optics and a AF488 filter (Carl Zeiss).

RNAi

Worms were synchronized by egg-laying and grown on plates seeded with HT115 carrying L4440 (control) or *glna-3* RNAi plasmid until the end of the experiment.[40]

RNA-seq

Worms were synchronized by hypochlorite treatment. ~6,000 L4 animals were collected, washed three times with M9 buffer, and frozen in Trizol (Ambion) at −80°C. RNA extraction was performed by lysing the worms through freeze-thaw in liquid nitrogen and 65°C water bath, followed by chloroform extraction and isopropanol precipitation. RNA samples were sequenced and analyzed by Novogene (Beijing, China). Three biological replicates were performed for both wild type and *glna(−)*.

Statistical overrepresentation analysis of GO terms and KEGG pathways associated with our entire RNA-seq dataset was performed using the DAVID functional annotation tool (https://david.ncifcrf.gov). WormBase IDs (WBGene000xxxxx) were entered for input and default p value calculation settings were used to determine significantly enriched GO terms and KEGG pathways.

Measurement of ROS

Endogenous ROS levels were measured using a ROS-sensitive probe H_2DCFDA.[41,42] Synchronized worms were collected and washed with M9 buffer. Worms were then incubated in M9 supplemented with 50 μM H_2DCFDA for 2 h at 37°C. Finally, they were observed under a Zeiss Imager M1 with a AF488 filter. Fluorescence intensity of individual worms was quantified using the ImageJ software.

NAC supplementation

NAC was added to the OP50 bacteria at a concentration of 2 mM. Worms were synchronized by egg-laying and grown on NGM plates seeded with NAC-supplemented OP50 until 1 dpL4 at 20°C.

QUANTIFICATION AND STATISTICAL ANALYSIS

Data are representative of at least two biological replicates. For body length analysis, n ≥ 21 animals; for fertility analysis, n ≥ 9 animals; for germline progenitor cell analysis, n ≥ 18 animals; for apoptosis analysis, n ≥ 21 animals; for oocyte size analysis, n ≥ 19 animals; for sperm number analysis, n ≥ 10 animals; for sperm size analysis, n ≥ 199 spermatids; for sperm activation experiments: n ≥ 7 animals; for ROS measurements, n ≥ 13 animals. Details of statistical analyses are reported in the figure legends. Statistical analyses were performed using GraphPad Prism and Adobe Illustrator was used to make figures.